Synthesis of MIL-53 Thin-films by Vapour-Assisted Conversion

Jan Warfsmann[a], Begum Tokay[a] * and Neil R. Champness[b] *

[a] Chemical and Environmental Engineering Department, Faculty of Engineering, University of Nottingham, University Park, Nottingham NG7 2RD, United Kingdom

[b] School of Chemistry, University Park, University of Nottingham, Nottingham, NG7 2RD, United Kingdom

Abstract

A simple method for the preparation of MIL-53 thin-films is reported. By employing a vapour-assisted conversion (VAC) approach we were able to prepare homogeneous MIL-53 films on a variety of glass, silicon or alumina substrates. Our strategy uses a vessel that allows film growth in an environment with a solvent-saturated atmosphere, in this case DMF. The VAC preparative conditions lead to the formation of a homogeneous film of the MOF and avoids the formation of alternative aggregates, such as starting materials. The effect of reaction temperature and time are investigated allowing identification of the optimum conditions to produce good film quality.

Introduction

Research into the properties of Metal-organic frameworks (MOFs) has grown over recent years as a result of their high porosity, adaptability and the due to the degree of design that can be applied to their synthesis in comparison with other typical porous materials such as zeolites, silica or activated carbon.[1,2] Consequently, they have received extensive interest in diverse fields including gas adsorption and separation,[3] controlled drug delivery,[4] catalysis[5] or in magnetic and electronic devices.[6,7] MOFs are in general first prepared as powder materials, but for several applications, the use of MOFs in thin-films with controllable chemical properties, morphology and thickness is advantageous. For example potential use of MOFs as membranes for gas separation,[8,9] sensing, where thin-films can improve signal transduction, sensitivity and selectivity[10] or catalysis, where a thin-film with controllable pore sizes can improve heat and mass transport.[11] The transfer of MOF powder synthesis to thin-film synthesis is often challenging. Whereas powder synthesis typically seeks to determine properties such as morphology or particle size, additional properties such as film thickness, roughness, particle distribution have to be controlled in order to create high quality thin-films. Furthermore, the formation of thin-films of MOFs is highly dependent on the specific MOF to be studied and the nature of the support and the interaction between the two will vary if porous Al_2O_3[12], flat glass surfaces,[13] stainless-steel mesh,[14] polymers,[15] foams[16] or other substrates are to be coated. The field of MOF thin-films becomes even more diverse with the introduction of free-standing MOF films or the usage of MOFs as a filler in polymer membranes as mixed-matrix membranes.[17] Consequently, numerous different approaches have been developed for possible thin-film synthesis of MOFs. Several methods have been adopted from the toolbox of the zeolite thin-film synthesis and the fields of MOF thin-films and zeolite thin-films continuously influence each other.[18] These methods can range from dip-coating,[19] Langmuir-Blodget techniques,[20] electrochemical methods[21] to more exotic methods such as the counter-diffusion approaches, where metal and linker solution diffuse into a porous membrane from separate sides[22] or the hot-pressing method, where a powder mixture of metal and linker precursor is placed on a support and reacts solvent-free to a thin-film by pressing with a heated stamp.[23] Amongst these strategies the Layer-by-Layer technique, which is also called liquid phase epitaxy (LPE)[24] has received much attention. This approach is based on the alternating immersion of

the support into metal and linker solution with washing steps with pure solvent between reactions to remove weakly attached species. In some instances, the film supports are further modified with self-assembled monolayers (SAMs)[25], which act as nucleation points for formation of the MOF thin-films. It is even possible to control the direction of growth of MOF thin-films.[26] However, a disadvantage of this approach is that long reaction times are typically needed to build up films of sufficient thickness and until now it was not reasonable to form films which a thickness of more than 100 nm, too thin for application such as membranes for gas separation,[27] although recent improvements to the LPE approach have been made by the application of automatization[28] or spray-coating.[27]

For the formation of thicker films in the micrometre range, alternative synthesis methods have been introduced. A direct in-situ approach is the most straightforward during which the support is immersed in a reaction mixture and a solvothermal synthesis conducted, similar to conventional powder synthesis. This technique has shown good results for some MOFs, e.g. MOF-5 on porous Al_2O_3,[29] or ZIF-8 on glass[13], but other reports show that the heterogenous nucleation of MOFs crystals on supports is not favoured and MOF particles are often difficult to attach to the surface.[30] As a possible method to improve nucleation of the MOF on the support a strategy of "seeding and secondary growth" has been developed.[31] Here, the surface is coated with small particles of the desired MOF[12] or starting material[32] which can lead to improved control of film morphology. Despite the widespread variety of MOFs most of the existing thin-film procedures have been applied for a few archetypical MOFs, such as ZIF-8 or HKUST-1, while for other MOFs methods to create thin-films are more sparse.

One of these MOFs is MIL-53, a porous material formed by $MO_4(OH_2)$ clusters (where M = Cr,[33] Al,[34] Fe[35] or Ga[36]) connected by 1,4-benzenedicarboxylate (BDC^{2-}), leading to a structure with one-dimensional rhombus-shaped channels. While the number of existing thin-film coatings is limited, MIL-53 has received considerable interest in research as a powder, in fields ranging from gas separation[37] and storage,[38] catalysis,[39] sensing[40] and water treatment.[41] This interest arises due to the unique features of MIL-53 including a breathing phenomenon, where the pore size of MIL-53 can reversibly change upon appropriate stimuli such as guest molecule absorption[34] or temperature variation.[42] Other attractive features include high thermal stability (up to 500 °C)[34] and the ability to vary both metal cation[33-36] and linker, through substitution of BDC[2,43-45] leading to a family of MOFs without changing the overall structure or morphology. Thus, the formation of MIL-53 thin-films may be advantageous for a number of applications, including as sensors or for gas separations. A approaches to the preparation of MIL-53 thin-films have been reported, but these have typically have the disadvantage of additional preparative steps, *e.g.* the secondary film growth with a preceding powder synthesis and the seeding step,[12] or the preparation only works on specific supports, *e.g.* aluminium sheets[46] or polyimide.[47]

Vapour Assisted Conversion (VAC) is an alternative strategy for thin-film synthesis. This method is related to other methods such as the dry-gel conversion or steam-assisted conversion[48] of zeolites, covalent organic frameworks (COF) or UiO-66.[49-51] The method involves placing a solid or precursor solution onto a support and then the system is exposed to solvent vapour, sometimes enriched with structure dictating agents as modulators. This approach can lead to the precise growth of a thin-film on various supports, often in shorter reaction times and at lower reaction temperatures in comparison with other existing thin-film synthesis methods. In this study, we show the first application of the VAC approach for the preparation of MIL-53 thin-films, resulting in the formation of homogenous thin-films in a single step and on non-modified supports such as glass, silicon or ceramic.

Experimental

$Al(NO_3)_3 \cdot 9H_2O$ and 1,4-benzenedicarboxylic acid, H_2BDC (>98%) were purchased from Sigma Aldrich. *N*,*N*-Dimethylformamide (DMF) and acetone were provided by Fischer-Scientific. All chemicals were

used without further purifications. Deionised water was collected from a Millipore Direct-Q 5 UV water purification system.

Methodology: The supports studied glass (soda-lime glass microscope slides; Fischer Scientific Menzel Gläser), silicon or Al_2O_3 were cut into pieces of 2 x 2 cm, immersed in acetone and cleaned by ultrasonication for 30 min. After ultrasonication, the glass slides were rinsed with deionised water and dried under a flow of N_2. The MIL-53 reaction mixture was prepared according to a previously published protocol[S1] as follows: a mixture of $Al(NO_3)_3{\cdot}9H_2O$ (5.99 mmol; 2.246 g) and H_2BDC (5.38 mmol; 0.895 g) were dissolved in DMF (30 ml), stirred vigorously at room temperature for 15 min until a clear solution was obtained. For the thin-film synthesis, a cleaned support was immersed in MIL-53 reaction mixture, extracted after 1 min, held vertically and excess reaction mixture drained off. For the reaction, the supports, wetted by MIL-53 reaction mixture, were placed vertically in the reaction vessel developed for the VAC (see Figure S7). For the Rapid Thermal Deposition (RTD) approach the samples were placed vertically on a petri dish. For either the VAC or RTD approach, the samples were placed in oven at a given reaction temperature (between 75 °C and 150 °C) over a reaction time between 1 h and 5 h. The sample was removed from the oven and allowed to cool naturally to room temperature.

Characterisation: X-Ray diffraction (XRD) measurements were performed using a Bruker D8 Advance diffractometer with a θ/θ goniometer geometry operated at 40 kV and 35 mA with Cu Kα radiation (λ = 1.540598 Å) with an exit slit of 0.6 mm diameter. A scintillation counter acted as X-Ray detector. The samples were scanned in the range between 5-35° 2θ with a step size of 0.02° and a step time of 10 s per step leading to a total measurement time of ~5 h. Scanning electron microscopy (SEM) was used to characterise the morphology and particle size (from an average of 25 particles) of the samples. Measurements were conducted using a Philips XL30 FEG ESEM or JEOL JSM-7100F FEG instrument with a beam voltage of 15 kV. The samples were sputtered with a 10 nm iridium film using a Quarum Q150T ES coater in order to increase the conductivity of the samples.

Results and Discussion

As a first attempt for the synthesis of MIL-53 films, the rapid thermal deposition (RTD) approach was investigated. Shah *et al.*[52] first applied the RTD approach for the formation of HKUST-1 and ZIF-8 thin-films using porous Al_2O_3 supports, but the strategy has subsequently been applied for the synthesis of MOF thin-films on glass.[53] For the RTD, a support is wetted with MOF precursor solution and the nucleation and growth of the thin-film induced by evaporation of the solvent.[54] While earlier thin-film reports used water as solvent for the synthesis of MIL-53,[12,46,47] we used DMF as reaction solvent for the RTD synthesis as DMF exhibits several advantages including higher yield[55] of the product MOF, called MIL-53(DMF) hereafter. Additionally, DMF dissolves both starting materials, $Al(NO_3)_3{\cdot}9H_2O$ and H_2BDC at room temperature, a prerequisite for the RTD approach. During our initial experiments thin-film coating of MIL-53 glass was used as the support (see Supporting Information for experimental details). We modified the approach reported by Shah *et al*[52] who reported the use of a high initial reaction temperature (up to 200 °C) for 15 minutes followed by slow cooling in the oven, a compromise between solvent evaporation and crystallization of the MOFs in order to form well-intergrown and crack-free films.[52] In our studies we did not find slow cooling to be beneficial for surface coverage and therefore (Figure S1) samples were therefore kept at reaction temperature during the whole process. SEM images of films created using the RTD approach reveal that this strategy does not lead to homogeneous coverage (Figure 1). Short reaction times led to the formation of particles with distinct sizes and morphologies. Thus, after 1 h reaction time (Figure 1a), the surface was covered with small angular particles (123 ± 31 nm) and larger triangular particles (430 ± 57 nm). After 3 h, the morphology of the surface coverage did not change (Figure 1b) but after 5 h the triangular particles disappeared

leaving visible gaps in the coating (Figure 1c). Indeed, only after prolonged reaction time (overnight reaction; ~17 h; Figure 1d) the surface was found to be completely covered with the angular particles.

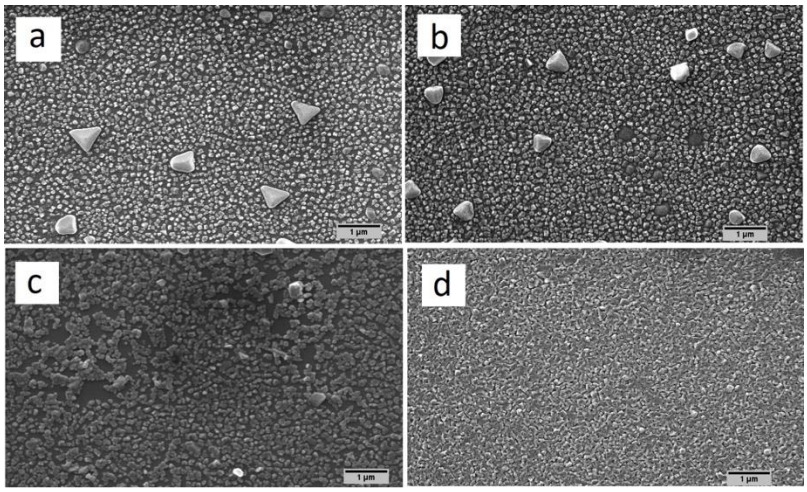

***Figure 1**: SEM images of glass slides covered by RTD after a) 1h, b) 3 h, c)5 h and overnight reaction (~17 h). Note the larger triangular particles at shorter reaction time which gradually disappear leaving gaps in the film coverage. Only after prolonged reaction times are more homogeneous films observed.*

Although these results were promising, the inhomogeneity of the films prepared was problematic. Figure 2 illustrates the problems encountered through a lower magnification SEM image of a film prepared on a glass slide prepared at 150 °C after 1 h reaction time. While the surface was partly covered with the above-mentioned angular shaped particles (Figure 2, highlighted in red) other parts of the surface were covered with leaf-shaped particles of ~5 µm in size (Figure 2, highlighted in blue). This leaf-shape was also observed for reference samples coated with pure H_2BDC (Figure S2) and even on a macroscopic scale can these areas with leaf-shaped particles be identified (Figure S6). Areas covered with angular particles were slightly opaque (in comparison to a transparent non-coated glass slide), while areas covered with leaf-shaped particles appeared bright white. These two types of particles could be identified on all coated glass slides regardless of the reaction time (Figure S3).

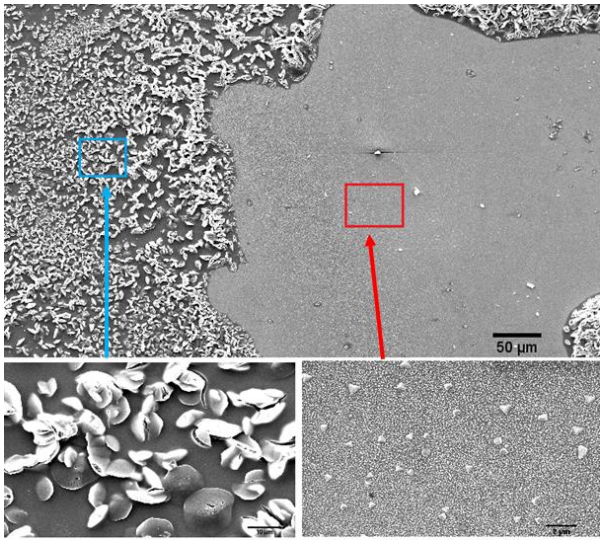

***Figure 2**: Image of glass slide covered by a film of MIL-53 using the RTD approach after 1 h at 150 °C. Two areas were visible on the surface. One area (red, bottom right) was covered with angular particles, while other areas (blue, bottom left) are covered with leaf-shaped particles.*

This observation was further confirmed by the measurement of XRD patterns of the films. A MIL-53 coated glass slide (RTD approach reaction time: 5 h/150 °C) was studied with diffraction patterns

recorded for different areas of the film; white area (Figure 3a) or opaque area (Figure 3b). The XRD pattern from the opaque area show a peak at 8.8°, which was in good agreement with the most intense peak of non-activated MIL-53(DMF).[57] Other peaks of MIL-53 were not visible in the pattern due to the thin depth of the coating. In contrast, an XRD-pattern measured for the white area (peaks at 17.4°, 25.2° and 27.9°) was in good agreement with the XRD pattern of the starting material H_2BDC. Hence, the formation of a thin-film of MIL-53 was only partly possible using the RTD-approach. The observation of unreacted starting material on the samples implied that the formation to MIL-53 stopped before complete conversion took place. In order to enable the formation of MIL-53, we concluded that either the evaporation of solvent had to be slowed or the reaction of MIL-53 required acceleration. Simply reducing the synthesis temperature (100 °C), in order to slow solvent evaporation, was unsuccessful and led to a sparsely covered surface containing cubic particles (Figure S3), and an XRD pattern, which has no peaks, which can be attributed to MIL-53(DMF) (Figure S4).

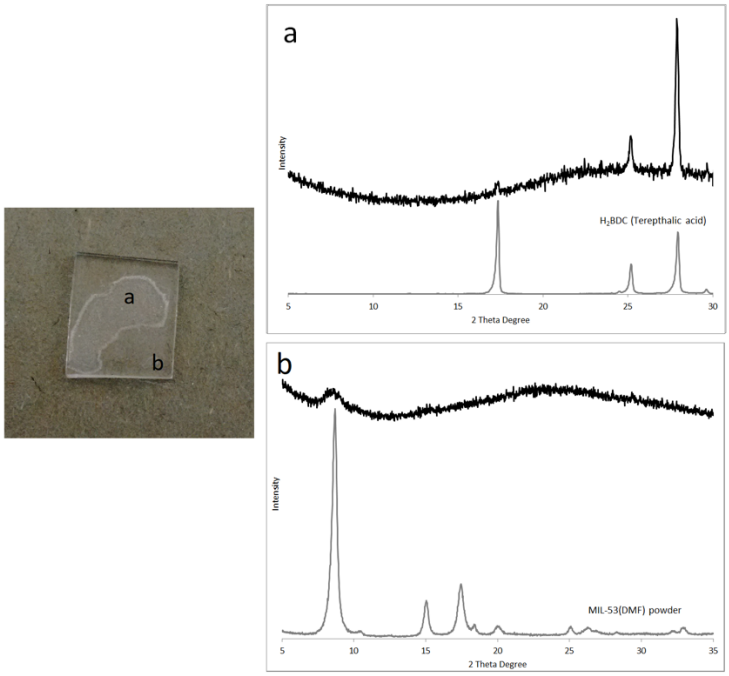

***Figure 3**: XRD patterns were recorded from RTD coated glass slide (5 h, 150 °C) at two positions. While the XRD pattern recorded from the white area "**a**" matched the pattern of the linker H_2BDC, in the pattern recorded at the opaque area "**b**" showed a peak at 8.8°, in good agreement with the pattern of MIL-53(DMF). The letters on the photo of the glass slide show the areas where the XRD-beam was focused.*

We hypothesised that a method to prevent the evaporation of the solvent in order to aid formation of homogeneous thin-films of the target MOF would be to perform the preparation in a saturated atmosphere of the solvent. In order to create such a saturated atmosphere, the reaction was conducted in an enclosed vessel which contains a reservoir of pure solvent. Such a set-up is similar to the vapour-assisted conversion (VAC), discussed above. Previous use of the VAC approach entailed a precise amount of solvent and modulator being allowed to diffuse into the reaction mixture and create a "reaction front" where the product is gradually formed.[48,56] In this study, however, the vapour is used to create a saturated atmosphere, which simply requires an excess of solvent, can be added to the reaction vessel. Thus, for the VAC reaction, the support, previously wetted with reaction mixture, was placed in a vessel specifically developed for this procedure (Figure S7). In short, a porcelain evaporation dish was placed in a larger glass crystallizing dish. The porcelain dish acts both as a support for a grid and as a reservoir for the solvent. The glass crystallizing dish was then covered with a lid and placed in

an oven to initiate the reaction at elevated temperature. This experimental set-up was not tightly sealed, but by choosing the appropriate temperature (up to 150 °C, B_p DMF: 153 °C) and adding sufficient solvent to the reservoir a saturated atmosphere can be maintained during the experiment. Figure 4 shows the photo of a glass slide, which was coated by VAC at 150 °C and 5 h reaction time, in comparison with a non-coated glass slide. Even on a macroscopic scale, the reaction by VAC has clearly led to a more homogenous coating of the surface in comparison with the previously investigated RTD-approach. The sample is homogenously coated, and no bright white areas are visible on the surface.

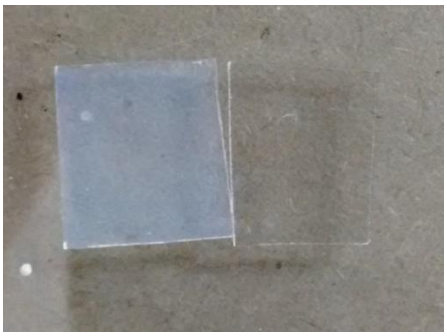

***Figure 4**: Image of a VAC-coated glass slide in comparison with a non-coated glass slide.*

In order to investigate the effect on the reaction temperature to the thin-film formation and to determine optimum reaction conditions, the reaction was first conducted at temperatures between 75 °C and 150 °C with a fixed reaction time of 5 h (Figure 5). Reaction at 75 °C resulted in a surface covered with leaf-shaped particles and an XRD pattern (Figure 6a) consistent with H_2BDC (peaks at 17.6°, 25.2° and 27.9°), implying that no reaction has taken place. In contrast was the glass slide at 100 °C reaction temperature covered with several tiles with a size ranging between 10 and 25 µm (Figure 5b). However, the XRD pattern for this sample gave no peaks, which can be attributed to starting material or MIL-53, suggesting amorphous material. At 125 °C the surface coverage was increased and only small gaps in the coating are visible (Figure 5c), while at 150 °C the surface was completely covered (Figure 5d). The XRD pattern of the samples prepared at both 125 °C and 150 °C showed peaks, which in in good agreement with a powder sample of MIL-53(DMF) (Figure 6c, 6d). Further analysis by SEM of a cross-section of the sample prepared at 150 °C reveals the thickness of the film to be approximately 4 µm (Figure 7). This SEM image further verified that the VAC approach led to a smooth and crack-free thin film coating on the support. In order to investigate the effect of the length of reaction on the thin-film formation the temperature was maintained at 150 °C and the reaction time was the reaction varied from 1 h to 3 h, see Figure 8 for SEM images and XRD pattern. With a reaction time of 1 h the surface was found to be only partially covered and the XRD pattern showed no peaks. Surface coverage was increased after a 3 h reaction time (Figure 8c), but in contrast to the glass slide prepared using a 5 h reaction time (Figure 5d), the surface coverage is still reduced, although the XRD pattern did confirm MIL-53(DMF) formation. The effectiveness of the approach was then extended to alternative supports and both ceramic and silicon could be successfully coated with MIL-53(DMF), verified by XRD (Figure 9) without the need for further surface modification. Interestingly the intensity of the diffraction is enhanced in the case of the film on ceramic suggesting enhanced crystallinity in this case.

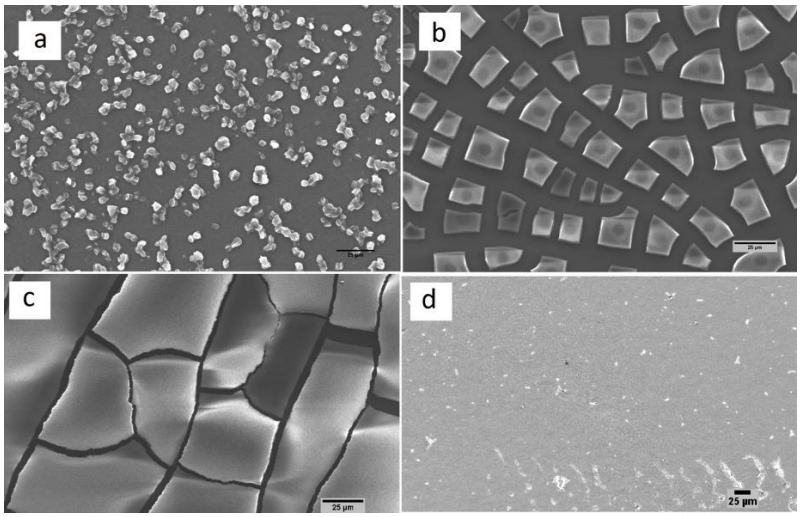

***Figure 5**: Images of samples prepared using the VAC coating approach with a fixed reaction time of 5 h and reaction temperature of a) 75 °C, b) 100 °C c) 125 °C and d) 150 °C.*

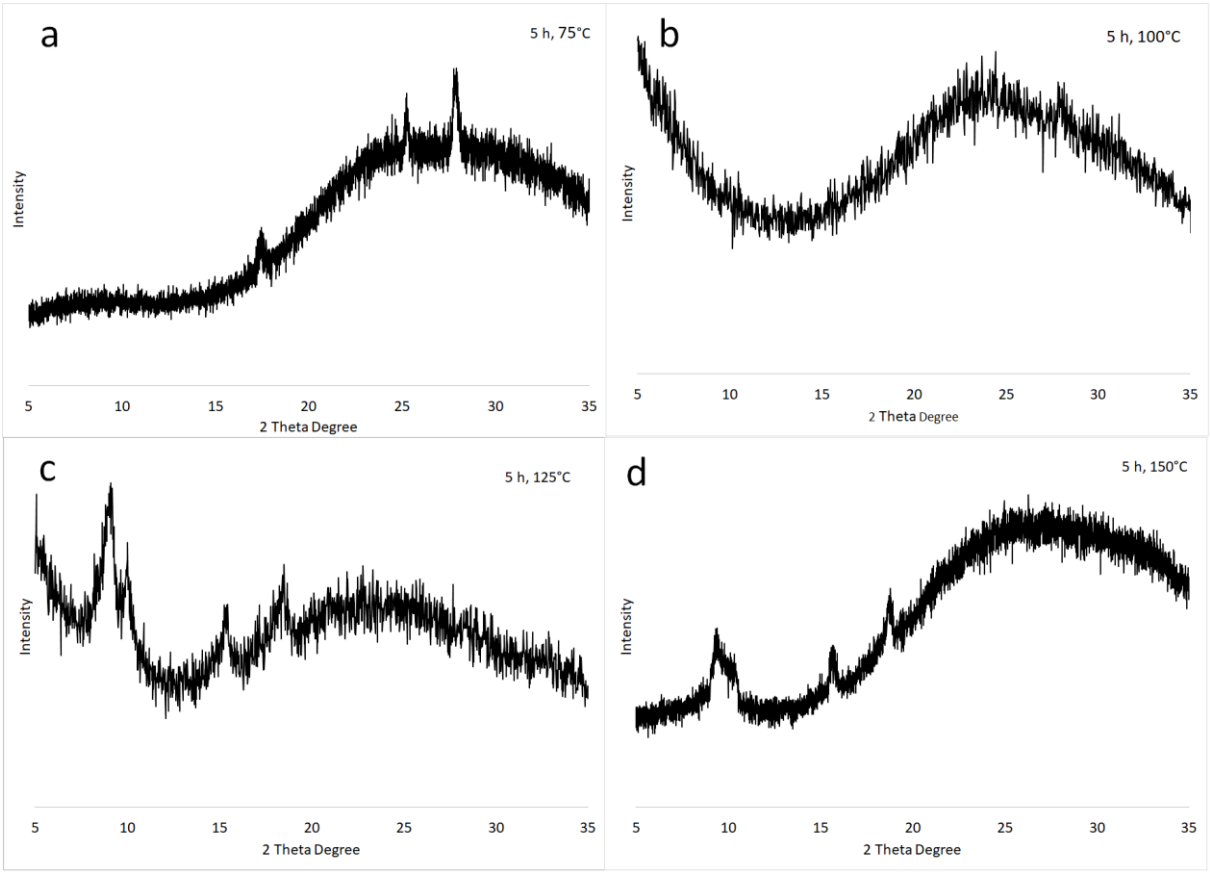

***Figure 6**: XRD pattern of the VAC coated glass slides at varying temperature. The XRD pattern of the slide coated at a) 75 °C was in good agreement with the pattern of the linker H_2BDC, while at b) 100°C no peaks were visible. The peaks of the glass slides covered at c) 125 °C and d) 150 °C show peaks matching with the typical pattern of MIL-53(DMF).*

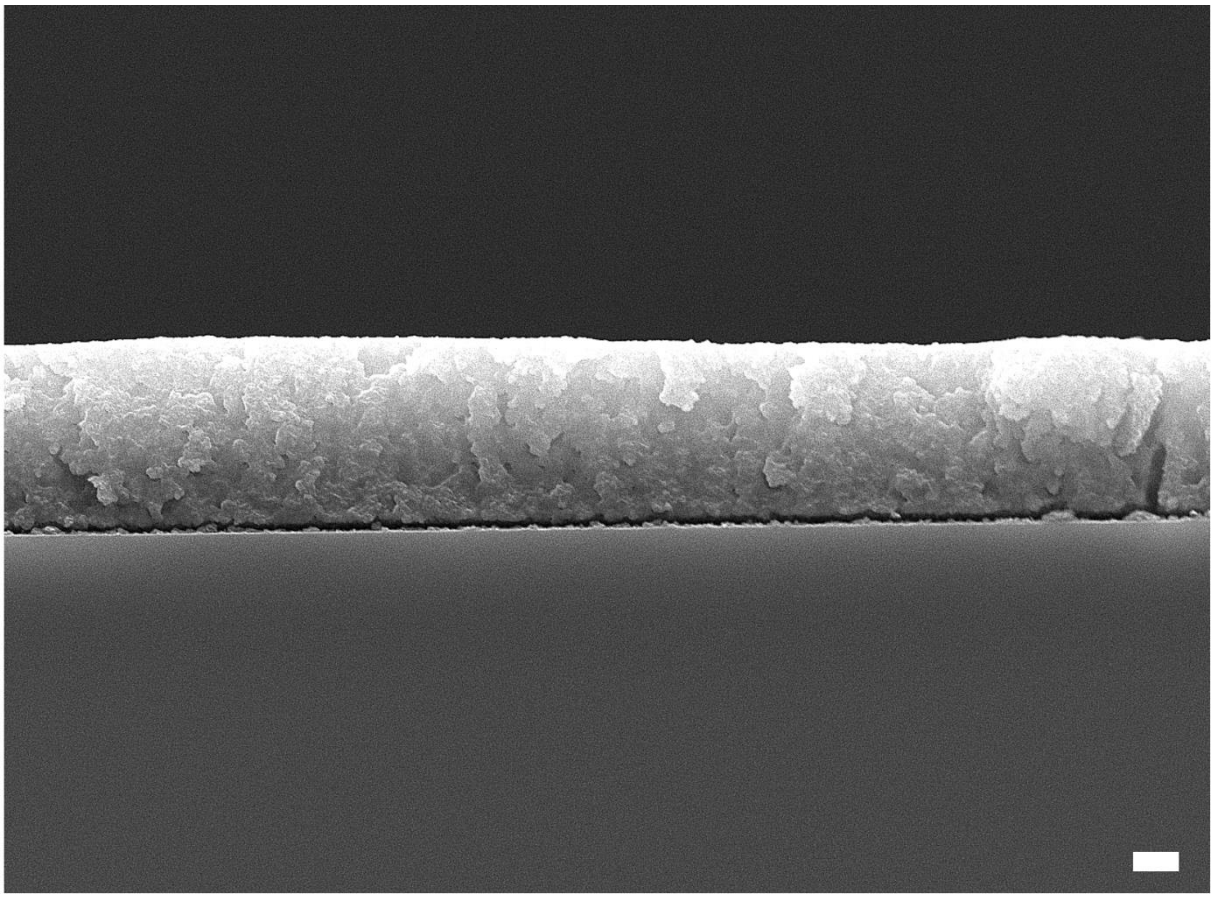

***Figure 7**: SEM side view of glass slide coated with MIL-53(DMF) using the VAC approach at 150 °C and 5 h reaction time. The resulting film has a thickness of 4 µm. The scale bar corresponds to 1 µm.*

Conclusion

In conclusion we have demonstrated a successful approach to preparing homogenous thin-films of MIL-53(DMF) using vapour-assisted conversion. Advantages of this approach are that no additional steps such as surface modification of the supports is necessary. Previous attempts to coat supports with MIL-53 by rapid-thermal deposition were unsuccessful, probably due to slower nucleation processes and reaction rates in comparison with other prototypical MOFs such as HKUST-1 or ZIF-8. However, preparing MIL-53 thin-films in a saturated atmosphere of DMF, at 150 °C and using a 5 h reaction time, led to the formation of homogenous, crack free thin-films. We anticipate that through appropriate modification the VAC approach will be applicable to other MOFs and on alternative supports.

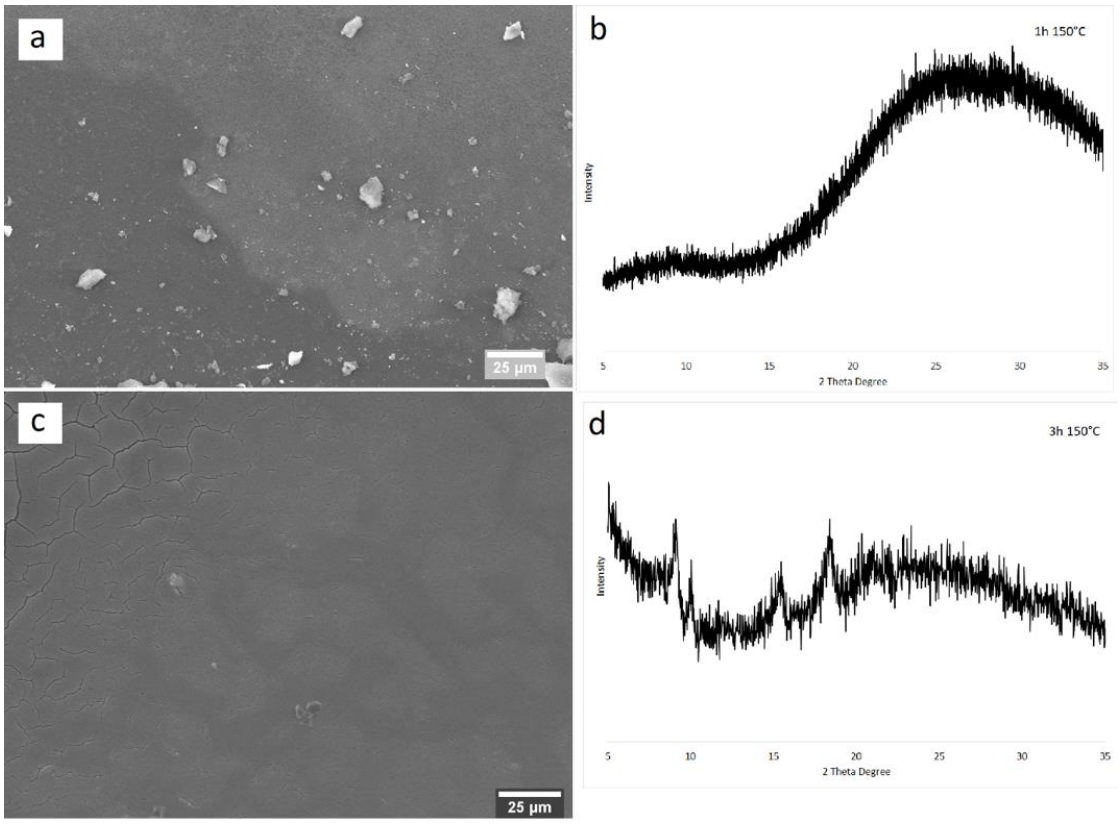

***Figure 8**: SEM image and XRD images of glass slides covered by VAC with 1 h reaction time (a, b) and after 3 h reaction time (c, d). The diffraction peaks in d) are consistent with MIL-53(DMF).*

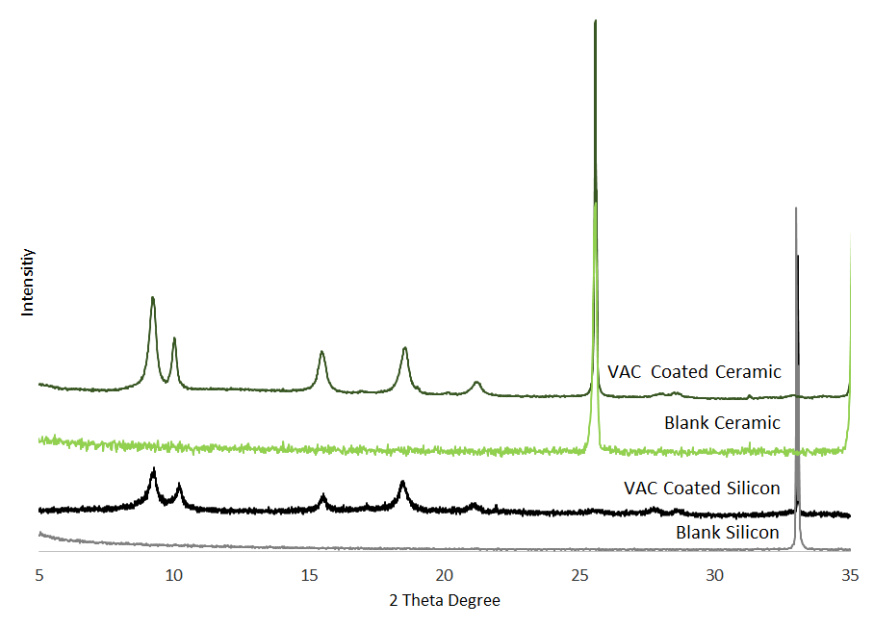

***Figure 9**: XRD images of blank silicon wafer before (grey) and Al_2O_3 support (light green) in comparison with supports coated with MIL-53(DMF) using the VAC approach; 5 h reaction time at 150 °C (black for silicon support and dark green for ceramic support). The coated pieces show diffraction peaks which can be attribute to MIL-53(DMF).*

Acknowledgement

This work was supported by the Engineering and Physical Sciences Research Council (EPSRC, EP/L022494/1). JW gratefully acknowledges receipt of a University of Nottingham Research Scholarship. The authors thank

the Nanoscale and Microscale Centre (nmRC) for providing access to instrumentation and Ms. Nicola J. Weston for assistance with ESEM.

References

1 S. Kitagawa, R. Kitaura and S.-i. Noro, *Angew. Chem. Int. Ed.*, 2004, **43**, 2334–2375.
2 R. Ricco, C. Pfeiffer, K. Sumida, C.J. Sumby, P. Falcaro, S. Furukawa, N.R. Champness and C.J. Doonan, *CrystEngComm*, 2016, **18**, 6532–6542.
3 J.-R. Li, R. J. Kuppler and H.-C. Zhou, *Chem Soc. Rev.*, 2009, **38**, 1477–1504.
4 R. C. Huxford, J. Della Rocca and W. Lin, *Curr. Opin. Chem. Bio.*, 2010, **14**, 262–268.
5 J. Lee, O. K. Farha, J. Roberts, K. A. Scheidt, S. T. Nguyen and J. T. Hupp, *Chem Soc. Rev.*, 2009, **38**, 1450–1459.
6 V. Stavila, A. A. Talin and M. D. Allendorf, *Chem. Soc. Rev.*, 2014, **43**, 5994–6010.
7 R. Ricco, L. Malfatti, M. Takahashi, A. J. Hill and P. Falcaro, *J. Mater. Chem. A*, 2013, **1**, 13033.
8 Y.-S. Li, F.-Y. Liang, H. Bux, A. Feldhoff, W.-S. Yang and J. Caro, *Angew. Chem. Int. Ed.*, 2010, **49**, 548–551.
9 Y. Yoo, Z. Lai and H.-K. Jeong, *Micro. Meso. Mat.*, 2009, **123**, 100–106.
10 G. Lu and J. T. Hupp, *J. Am. Chem. Soc.*, 2010, **132**, 7832–7833.
11 J. Hedlund, O. Öhrman, V. Msimang, E. van Steen, W. Böhringer, S. Sibya and K. Möller, *Chem. Eng. Sci.*, 2004, **59**, 2647–2657.
12 H. Fan, H. Xia, C. Kong and L. Chen, *Int. J. Hydrogen Ener.*, 2013, **38**, 10795–10801.
13 G. Lu, O. K. Farha, W. Zhang, F. Huo and J. T. Hupp, *Adv. Mater.*, 2012, **24**, 3970–3974.
14 J. W. Maina, J. A. Schütz, L. Grundy, E. Des Ligneris, Z. Yi, L. Kong, C. Pozo-Gonzalo, M. Ionescu and L. F. Dumée, *ACS Appl. Mater. Inter.*, 2017, **9**, 35010–35017.
15 A. M. Ullman, C. G. Jones, F. P. Doty, V. Stavila, A. A. Talin and M. D. Allendorf, *ACS Appl. Mater. Inter.*, 2018, **10**, 24201–24208.
16 O. Shekhah, L. Fu, R. Sougrat, Y. Belmabkhout, A. J. Cairns, E. P. Giannelis and M. Eddaoudi, *Chem. Commun.*, 2012, **48**, 11434–11436.
17 T.-S. Chung, L. Y. Jiang, Y. Li and S. Kulprathipanja, *Prog. Polym. Sci.*, 2007, **32**, 483–507.
18 N. Rangnekar, N. Mittal, B. Elyassi, J. Caro and M. Tsapatsis, *Chem. Soc. Rev.*, 2015, **44**, 7128–7154.
19 A. Demessence, C. Boissière, D. Grosso, P. Horcajada, C. Serre, G. Férey, Soler-Illia, Galo J. A. A. and C. Sanchez, *J. Mater. Chem.*, 2010, **20**, 7676.
20 R. Makiura, S. Motoyama, Y. Umemura, H. Yamanaka, O. Sakata and H. Kitagawa, *Nat. Mat.*, 2010, **9**, 565–571.
21 W.-J. Li, M. Tu, R. Cao and R. A. Fischer, *J. Mater. Chem. A*, 2016, **4**, 12356–12369.
22 H. T. Kwon and H.-K. Jeong, *J. Am. Chem. Soc.*, 2013, **135**, 10763–10768.
23 S. Rackley, *Carbon Capture and Storage*, Elsevier professional, s.l., 1st edn., 2009.
24 B. Liu and R. A. Fischer, *Sci. China Chem.*, 2011, **54**, 1851–1866.
25 J. C. Love, L. A. Estroff, J. K. Kriebel, R. G. Nuzzo and G. M. Whitesides, *Chem. Rev.*, 2005, **105**, 1103–1169.
26 E. Biemmi, C. Scherb and T. Bein, *J. Am. Chem. Soc.*, 2007, **129**, 8054–8055.
27 H. K. Arslan, O. Shekhah, J. Wohlgemuth, M. Franzreb, R. A. Fischer and C. Wöll, *Adv. Funct. Mater.*, 2011, **21**, 4228–4231.
28 Z.-G. Gu, A. Pfriem, S. Hamsch, H. Breitwieser, J. Wohlgemuth, L. Heinke, H. Gliemann and C. Wöll, *Micro. Meso. Mat.*, 2015, **211**, 82–87.
29 Y. Liu, Z. Ng, E. A. Khan, H.-K. Jeong, C.-b. Ching and Z. Lai, *Micro. Meso. Mat.*, 2009, **118**, 296–301.

30 Z. Liao, T. Xia, E. Yu and Y. Cui, *Crystals*, 2018, **8**, 338.
31 V. V. Guerrero, Y. Yoo, M. C. McCarthy and H.-K. Jeong, *J. Mater. Chem.*, 2010, **20**, 3938.
32 Y. Hu, X. Dong, J. Nan, W. Jin, X. Ren, N. Xu and Y. M. Lee, *Chem. Commun.*, 2011, **47**, 737–739.
33 G. Férey, M. Latroche, C. Serre, F. Millange, T. Loiseau and A. Percheron-Guégan, *Chem. Commun.*, 2003, 2976–2977.
34 T. Loiseau, C. Serre, C. Huguenard, G. Fink, F. Taulelle, M. Henry, T. Bataille and G. Ferey, *Chem. Eur. J.*, 2004, **10**, 1373–1382.
35 T. Devic, F. Salles, S. Bourrelly, B. Moulin, G. Maurin, P. Horcajada, C. Serre, A. Vimont, J.-C. Lavalley, H. Leclerc, G. Clet, M. Daturi, P. L. Llewellyn, Y. Filinchuk and G. Férey, *J. Mater. Chem.*, 2012, **22**, 10266.
36 C. Volkringer, T. Loiseau, N. Guillou, G. Ferey, E. Elkaim and A. Vimont, *Dalton Trans.*, 2009, 2241–2249.
37 P. Serra-Crespo, T. A. Wezendonk, C. Bach-Samario, N. Sundar, K. Verouden, M. Zweemer, J. Gascon, H. van den Berg and F. Kapteijn, *Chem. Eng. Technol.*, 2015, **38**, 1183–1194.
38 K. Akhbari and A. Morsali, *Mat. Lett.*, 2015, **141**, 315–318.
39 F. fMartínez, G. Orcajo, D. Briones, P. Leo and G. Calleja, *Micro Meso Mat*, 2017, **246**, 43–50.
40 C.-X. Yang, H.-B. Ren and X.-P. Yan, *Anal. Chem.*, 2013, **85**, 7441–7446.
41 L. Paseta, E. Simón-Gaudó, F. Gracia-Gorría and J. Coronas, *Chem. Eng. J.*, 2016, **292**, 28–34.
42 M. Mendt, B. Jee, N. Stock, T. Ahnfeldt, M. Hartmann, D. Himsl and A. Pöppl, *J. Phys. Chem. C*, 2010, **114**, 19443–19451.
43 J. Gascon, U. Aktay, M. Hernandez-Alonso, G. van Klink and F. Kapteijn, *J. Catal.*, 2009, **261**, 75–87.
44 S. Biswas, T. Ahnfeldt and N. Stock, *Inorg. Chem.*, 2011, **50**, 9518–9526.
45 J. Yang, X. Yan, T. Xue and Y. Liu, *RSC Adv*, 2016, **6**, 55266–55271.
46 F. Zhang, X. Zou, F. Sun, H. Ren, Y. Jiang and G. Zhu, *CrystEngComm*, 2012, **14**, 5487–5492.
47 T. Tsuruoka, M. Kumano, K. Mantani, T. Matsuyama, A. Miyanaga, T. Ohhashi, Y. Takashima, H. Minami, T. Suzuki, K. Imagawa and K. Akamatsu, *Crystal Growth & Design*, 2016, **16**, 2472–2476.
48 M. Matsukata, M. Ogura, T. Osaki, Hari Prasad Rao, Poladi Raja, M. Nomura and E. Kikuchi, *Top. Catal.*, 1999, **9**, 77–92.
49 K. Möller, B. Yilmaz, R. M. Jacubinas, U. Müller and T. Bein, *J. Am. Chem. Soc.*, 2011, **133**, 5284–5295.
50 D. D. Medina, J. M. Rotter, Y. Hu, M. Dogru, V. Werner, F. Auras, J. T. Markiewicz, P. Knochel and T. Bein, *J. Am. Chem. Soc.*, 2015, **137**, 1016–1019.
51 E. Virmani, J. M. Rotter, A. Mähringer, T. von Zons, A. Godt, T. Bein, S. Wuttke and D. D. Medina, *J. Am. Chem. Soc.*, 2018, **140**, 4812–4819.
52 M. Shah, H. T. Kwon, V. Tran, S. Sachdeva and H.-K. Jeong, *Micro. Meso. Mat.*, 2013, **165**, 63–69.
53 J. Hromadka, B. Tokay, R. Correia, S. P. Morgan and S. Korposh, *Sensor Actuat B - Chem*, 2018, **255**, 2483–2494.
54 R. Ameloot, E. Gobechiya, H. Uji-i, J. A. Martens, J. Hofkens, L. Alaerts, B. F. Sels and D. E. de Vos, *Adv. Mater.*, 2010, **22**, 2685–2688.
55 X. Cheng, A. Zhang, K. Hou, M. Liu, Y. Wang, C. Song, G. Zhang and X. Guo, *Dalton Trans.*, 2013, **42**, 13698–13705.
56 A. L. Semrau, S. Wannapaiboon, S. P. Pujari, P. Vervoorts, B. Albada, H. Zuilhof and R. A. Fischer, *Cryst. Growth Des.*, 2019, **19**, 1738–1747.
57 J. Warfsmann, B. Tokay and N. R. Champness, *CrystEngComm*, 2018, **20**, 4666–4675.

Table of Contents Entry

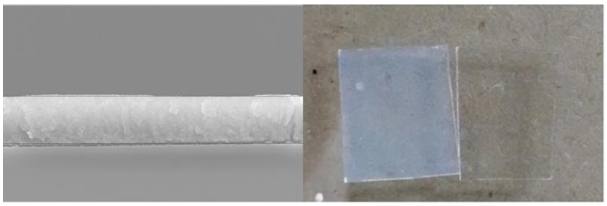

Using a vapour-assisted conversion approach it is possible to prepare homogeneous MIL-53 thin-films on a variety of substrates.